

# Synthesis, Characterization of Cu-Ni-Sn-P-(Ga) Based Amorphous Alloys, and the Development of Their Applications Using Specific Hybrid Additive Manufacturing Processes

## **Ph.D.** Thesis – Abstract

for obtaining the scientific title of doctor at Universitatea Politehnica Timișoara in the doctoral field Materials <u>Engineering</u>

Author: Ing. Sebastian AMBRUS

scientific supervisor Prof.univ.dr.ing. Viorel-Aurel ŞERBAN

#### **Chapter 1 Introduction**

Amorphous metal alloys, also called metal glasses in the particular case of obtaining by ultra-fast cooling of the melt, have aroused increasing interest in recent decades, both from a scientific perspective and in terms of their application potential. The special properties of these materials have been the basis for the expansion of the fields of use, favoring the development of varied and innovative applications. Depending on their chemical composition, we find them in uses that require the most diverse operating properties: from precision micro mechanical components (which must have high values of mechanical strength, ductility, corrosion resistance, wear resistance, vibration resistance), to electronic components (which involve specific magnetic and electrical properties) or aerospace components (which must withstand extreme temperatures and pressures), security systems, medical applications even the sports equipment industry (from golf clubs to tennis rackets).

In this sense, the use of metal bottles in the manufacture of components from polymer matrix composites reinforced with particles or strips has represented a new direction of success in order to improve their behavior in the different applications in which they are used.

Even if the expansion of the forms under which amorphous structures can be obtained has registered a spectacular leap from strips and wires to fruits and "bulks", the dimensional limitations due to the elaboration processes are still a major impediment in diversifying the uses of these materials in areas where their properties would contribute to the relevant improvement of the product characteristics.

The present paper aims to broaden the application spectrum of these amorphous metal alloys by resorting to various manufacturing methods that belong to the concept of Hybrid Additive Manufacturing.

Hybrid additive manufacturing is actually a development of additive manufacturing methods.

Additive manufacturing, commonly known as 3D printing, has as its principle of making an object the construction layer by layer starting directly from a CAD model. These techniques allow the creation of complex geometries without material loss. The negative aspects of a lower surface roughness, residual stresses and mechanical properties affect the performance of this method.

Hybrid additive manufacturing of materials consists of introducing conventional manufacturing methods into the manufacturing cycle by combining them with additive manufacturing techniques in order to improve the quality of products of high complexity and superior performance.

The research in the present paper focused on the Cu-Ni-Sn-P family of non-ferrous alloys.

New technologies in the fields of computer science and electronics, as well as those in the automotive, aeronautical and aerospace industries have revealed the role and importance of the new families of non-ferrous alloys. Among the copper alloys in demand in these areas, the best performing is the high-strength and elastic alloy Cu-Be. The limitations due to toxicity and high costs led to the development of new families with similar properties from which the Cu-Ni-Sn family of alloys stands out. The most representative alloy Cu-15Ni-8Sn has exceptional elastic properties: mechanical strength and very good hardness, wear and corrosion resistance.



At certain chemical compositions and technological processes, these alloys have a high capacity for forming amorphous structures (GFA - Glass Forming Ability).

Thus, Cu–Sn–Ni–P-based metal bottles can be obtained relatively easily in various forms, such as wires, strips or even massive products with a thickness of 1–3 mm, by pouring the melt into suitable molds. As a result of its outstanding properties in the amorphous state (excellent electrical and thermal conductivity, mechanical strength, high corrosion and wear resistance, etc.), they can be successfully used widely in the aerospace, electronics and mechanical industries.

#### **Chapter 2 State of the art**

#### **Amorphous metallic alloys**

Disordered structures, especially amorphous ones, still have exceptional potential for development, especially in that of applications in the new cutting-edge areas of industry. Although in terms of production they have already reached the 3rd generation, and some of their developments, such as dealloyed nanoporous structures, have found applications in the field of microelectronics, sensors, etc. It is believed that there is still a huge untapped technological potential with the implementation of new manufacturing technologies.

An amorphous alloy is generally structurally a monophasic material (100% amorphous structure). Amorphous metal alloys, which are characterized by a lack of atomic arrangement over long distances, exhibit a high yield strength, excellent mechanical strength, high thermoplasticity, and good corrosion resistance. After the discovery of amorphous alloys, more than 60 years ago, the interest in such materials increased significantly, even if the geometric dimensions obtained, limited by the preservation of the amorphous structure, represented an impediment.[1], [2], [3], [4]

In recent years, through the development of new technologies, a large number of metal alloys based on Zr, Mg, La, Ti, Fe, Cu and Ni have been made in the form of amorphous bars with dimensions ranging from a few millimeters to a few centimeters.[2], [5]

Amorphous metal alloys obtained by ultra-fast cooling of melts are referred to as metal bottles. Through this rapid solidification, the atoms in the structure are locked in their configuration from the liquid state and thus avoid the formation of an orderly arrangement in space. However, at small interatomic distances, a certain orderly arrangement of atoms can be observed. In recent years, these alloys have seen a significant expansion of use in multiple industrial sectors, including aerospace, automotive, as well as electrical and electronic engineering.[6]

#### Glass forming ability

One of the biggest challenges in obtaining massive amorphous alloys is their ability to form an amorphous structure, a property known as glass forming ability (GFA) [7]. This capability is essential for the development of metallic materials with improved functional properties, and a thorough understanding of the mechanisms involved in the formation of amorphous structure is a fundamental step in the advancement of this field. Amorphization capacity designates the ease with which a metallic liquid can be cooled in a way that prevents nucleation and the growth of crystalline phases. This is decisively influenced by the chemical composition of the alloy, as well as by the methods and technological conditions applied in the solidification process. [8].

In the context of devitrification, the amorphization capacity of a system can be evaluated either by means of the critical cooling rate (Rc) or by the maximum size of the amorphous sample obtained (Dmax). A lower value of the critical cooling rate or a larger maximum diameter of the amorphous sample reflects a higher capacity for amorphous phase formation. However, the precise experimental determination of the cooling rate is difficult to achieve, and the value of the maximum size obtained is significantly influenced by the elaboration technology used [9].

Previous studies have mainly focused on identifying the structural and thermodynamic factors influencing the formation of the amorphous phase under rapid cooling conditions. However, the kinetic influences of the process have been largely neglected. In addition, the criteria proposed in the literature are often difficult to apply in practice, which limits their effectiveness as predictive tools for the selection of optimal chemical compositions in order to obtain the amorphous structure.



Subsequently, the analysis of the amorphization capacity of various alloys was extended by taking into account kinetic parameters, such as nucleation rate, crystal growth rate and phase transformation dynamics. These approaches have led to significant advances in understanding the physical mechanisms involved in the formation of massive amorphous alloys. Among the aspects studied are the crystallization processes, the influence of the alloying elements, the rheological behavior of the melt (especially its viscosity), as well as the mechanisms of formation of the amorphous structure at the macro- and microscopic scale. [10], [11].

Based on the characteristic temperatures and other physical properties of the amorphous alloys, a number of additional parameters have been proposed for the evaluation of the amorphization capacity. A notable example is the low glass transition temperature, Trg (defined as the ratio of the glass transition temperature, Tg, and the melting temperature, Tl, introduced by Turnbull. However, it is important to emphasize that this parameter was originally designed for monatomic systems, which reduces its relevance in the case of multicomponent alloys. In a later approach, Lu's research showed that the inverse ratio, Tl/Tg, shows a more faithful correlation with the amorphisation capacity in the case of multicomponent systems, thus providing a more appropriate criterion for assessing the potential for metal glass formation. [12], [13]

One of the criteria frequently used to evaluate the amorphization capacity is the one proposed by Inoue, who formulated a set of empirical rules aimed at favoring the formation of massive amorphous alloys. These four rules – which include the existence of at least three components, significant differences between the atomic radii of the constituent elements, the enthalpy of negative mixing and a complex structure of the atomic lattice – help to identify compositions with a high potential for amorphous phase formation. The application of these criteria provides a useful framework for the design and selection of alloys with good metal glass formability: [14]

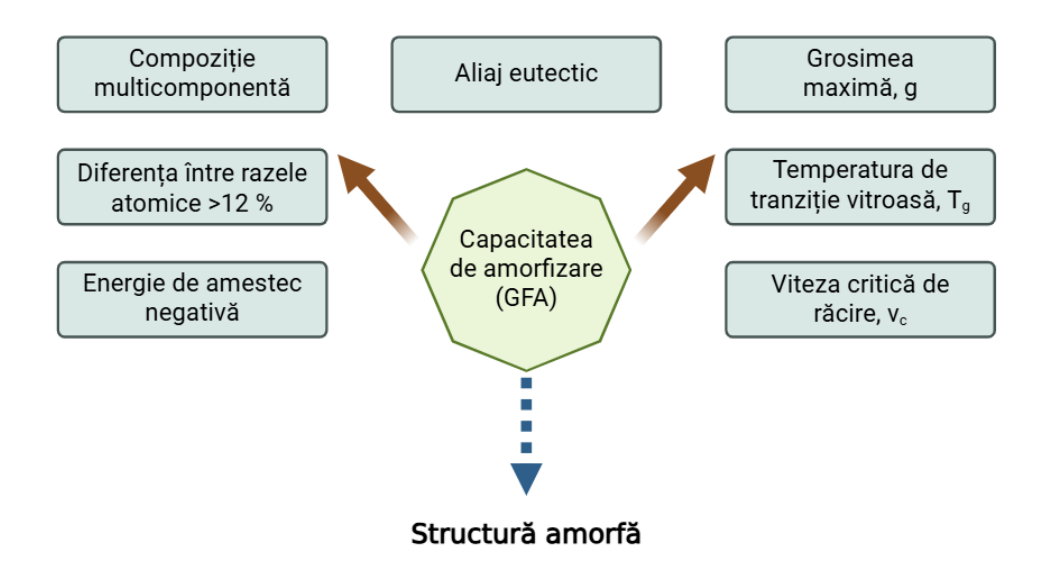


Figure 1 Parameters influencing amorphization capacity

#### Methods and procedures for obtaining

The diagram of a technological itinerary for obtaining products with an amorphous structure is illustrated in the following figure:



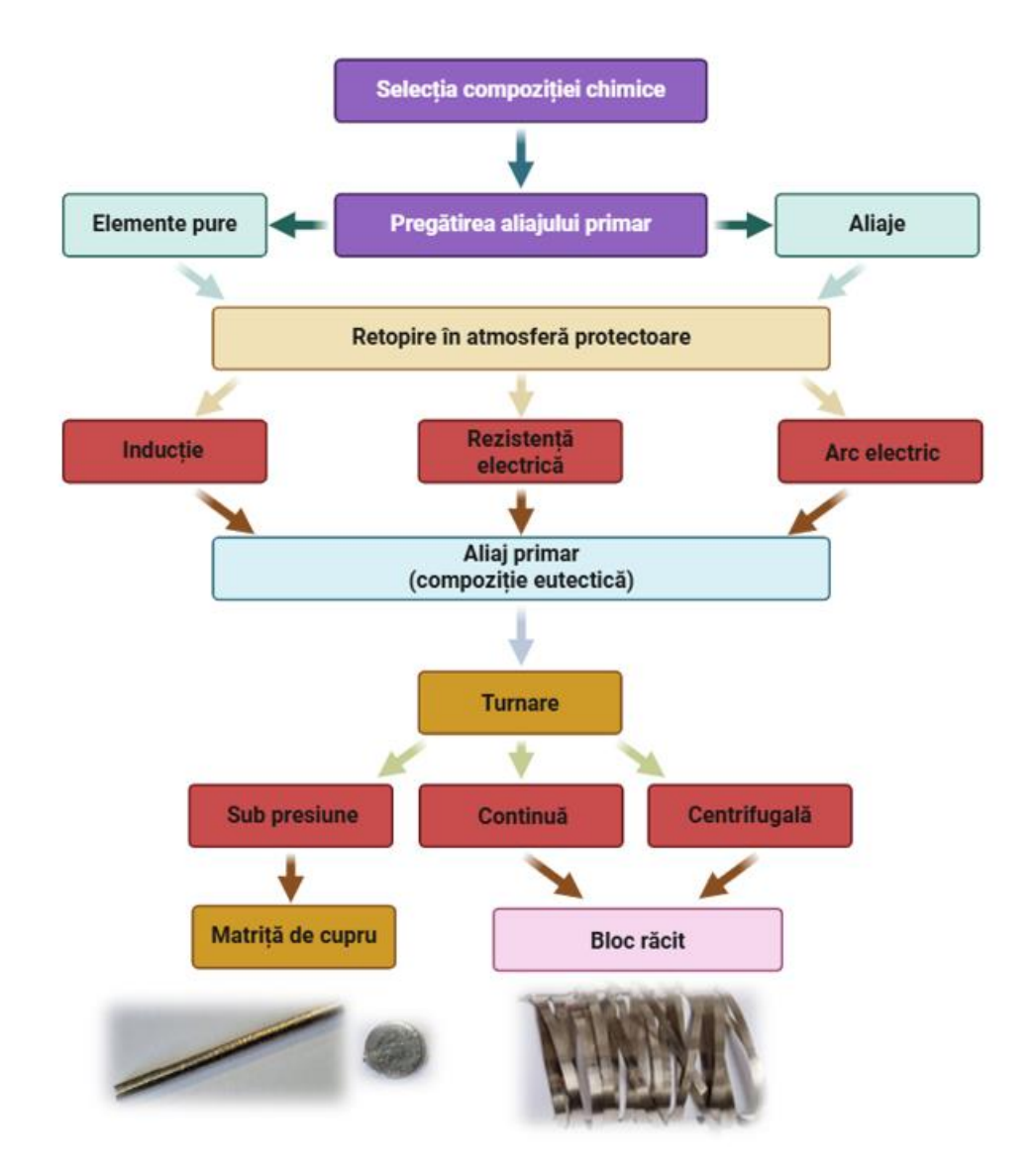


Figure 2 Schematic representation of the technological itinerary for the elaboration of amorphous alloy products, highlighting the main melting and casting processes

Amorphous metal alloys can be obtained through a wide range of technological methods and processes. Among the most used are mechanical alloying, rapid solidification from melting, irradiation, ion implantation, laser processing, PVD and CVD deposition, electrolytic deposition, thermal spraying, as well as the application of high pressures. Regardless of the method used, the common goal is to increase the free energy of the system (by increasing the temperature, pressure or by introducing mechanical energy), followed by rapid cooling of the material to preserve the metastable phase or using this state as an intermediate step in obtaining the desired microstructure and properties.

#### Continuous methods for obtaining amorphous metal alloys in the form of ribbons

The production of metal alloys by liquid-phase solidification, using continuous methods, has made significant progress in recent decades. These techniques make it possible to obtain products with homogeneous properties, controlled dimensions and geometries adapted to the requirements of industrial applications. Although the cooling rates characteristic of these methods (approximately 10<sup>6</sup>)



K/s) are lower compared to those of conventional ultra-fast cooling processing, they are often sufficient to achieve the amorphous phase in many alloy systems.

A critical aspect in the development of continuous amorphous fibers or strips is the stabilization of the liquid jet before solidification. Alloys that can be easily drawn from the melt generally exhibit high viscosity and low surface tension, characteristics that help maintain the coherence of the metal jet. On the other hand, alloys with low viscosity and high surface tension tend to generate instabilities in the jet, favoring its fragmentation into droplets and thus preventing the continuous formation of the amorphous product.

#### **Melt-spinning method**

The Melt-spinning process is a method used for the rapid solidification of certain alloys, mainly to obtain amorphous metal strips or so-called "metal bottles", which cannot be manufactured using conventional continuous casting processes. Depending on the centrifugation conditions, amorphous structures can be obtained due to the extremely high cooling speeds. In this process, first an alloy is melted inside a crucible and then with the help of an inert gas, the melt is discharged through a nozzle located at the bottom of the crucible directly onto the cooling roller, made of copper, where it solidifies instantly.

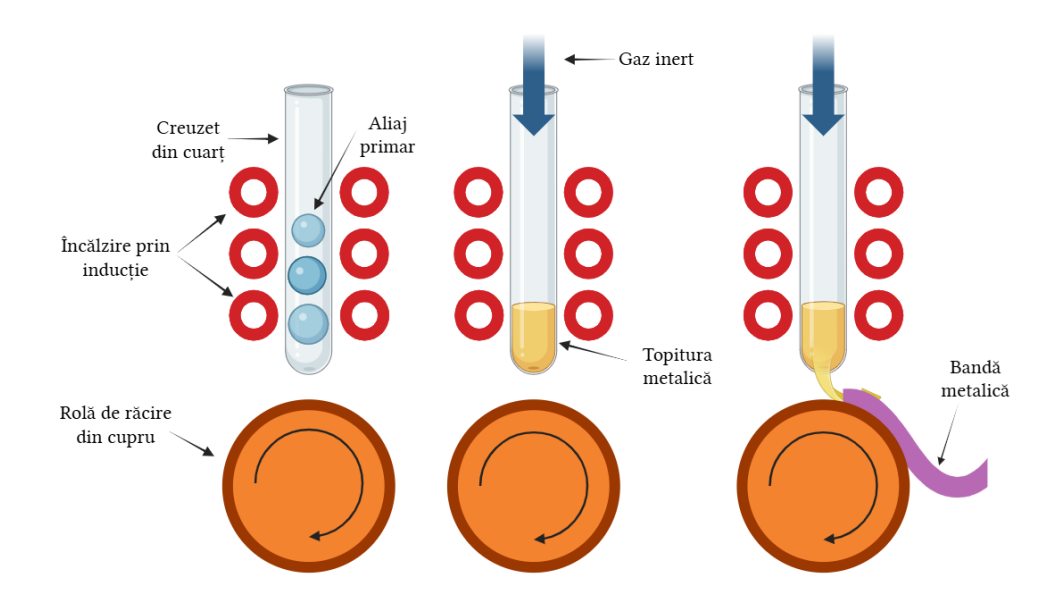


Figure 3 Graphic demonstration of the steps taken in the Melt Spinning process[15]

This process is an extremely complex one in which the rotation speed of the cooling roller, the melt outlet pressure, the nozzle-cooling roller distance and the melting temperature are the most important parameters. However, there are other parameters that can affect the shape, uniformity, grain size and quality of the final surface, such as the geometry of the nozzle, the roughness of the wheel surface, whether the process is carried out in air or vacuum, and even the type of gas used to discharge the melt.[15]

#### Solidification method between two rollers

In this method, illustrated in the adjacent figure, the melt jet is forced to pass between two rotating rollers. Upon contact with the cold surfaces of the rollers, the melt is rapidly cooled, which leads to the formation of a strip of uniform thickness.



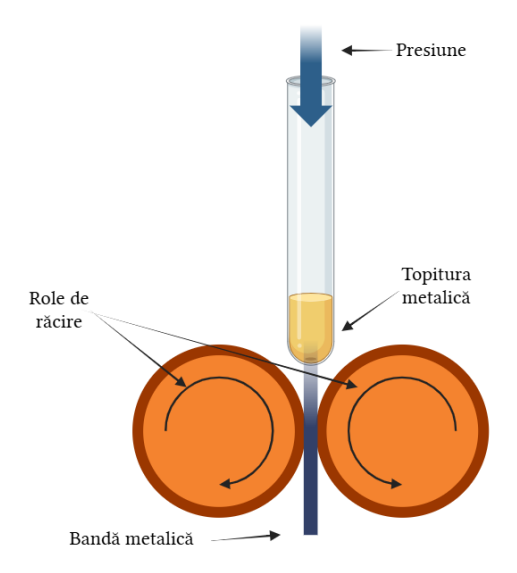


Figure 4 Principle diagram of the solidification method between two rollers

An essential condition for the successful achievement of amorphous metal strips by rapid solidification methods is the synchronization of the output speed of the liquid jet from the crucible hole with the solidification rate. For the elaboration of very small strips, cooling rollers pressed together are used, which ensures efficient thermal contact. The surfaces of these rolls must have a high hardness and be ground with high precision, in order to allow the formation of strips with uniform and constant thicknesses.

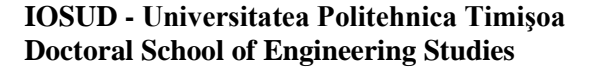
The contact time of the melt with the cooling surface is extremely short, and then the metal strip continues the process of cooling in the air, by radiation and convection. During this rapid solidification method, the strip can suffer deformations both during solidification and in the subsequent cooling step, as a result of mechanical compressive stresses. These internal stresses can lead, in some cases, to cracks on the surface of the belt.

#### Planar flow casting method

Obtaining amorphous alloys on an industrial scale is only possible by using continuous rapid cooling processes (Figure X). Within these technologies, the primary alloy, initially with a crystalline structure and chemical composition optimized for amorphization, is melted by induction in a crucible made of quartz. The resulting melt is then forced through the slot of an ejector nozzle, settling on the surface of a rotating cylinder.

The direct contact of the liquid jet with the cold surface of the moving cylinder causes the ultra-fast solidification of the alloy, favoring the formation of the amorphous structure in the form of a thin metal strip.

.





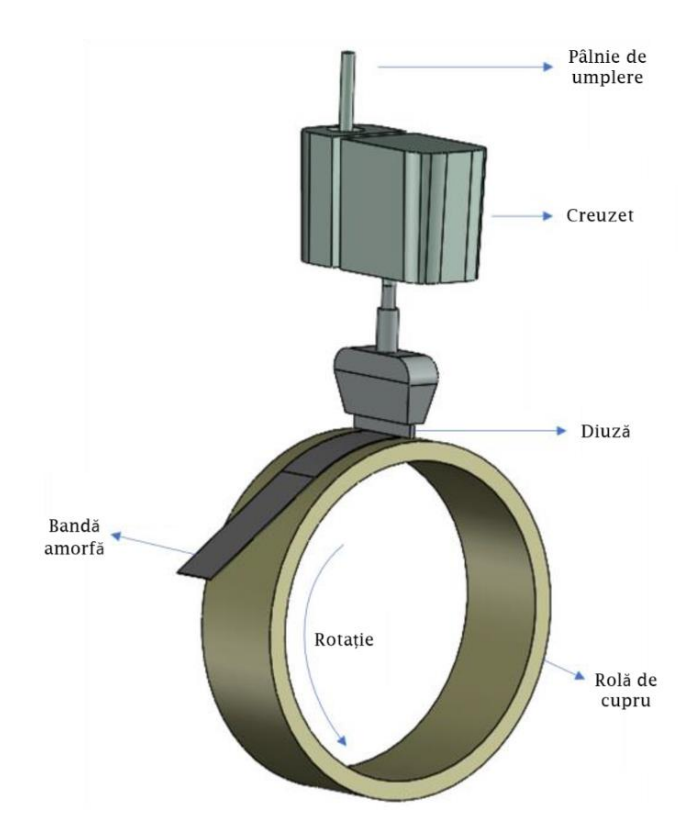


Figure 5 Principle diagram of the planar flow casting method[16]

In this method, the ejection nozzle is positioned at a very small distance from the cooling surface — usually under one millimeter — which allows for effective mechanical stress of the metal bath and helps to reduce disturbances during solidification. Ultra-fast cooling of the melt on the surface of a rotating cylinder enables outstanding technological performance. Through this technique, amorphous metal strips with large widths (between 20 and 100 mm) can be obtained under conditions of high efficiency and stability.

#### Properties of amorphous metal alloys

Amorphous metal alloys are distinguished by a set of exceptional mechanical properties that are difficult to find in other classes of materials. The absence of the crystal structure leads to high mechanical strength, easy magnetization, low attenuation of acoustic waves, as well as increased electrical resistivity. Also, the structural homogeneity, associated with an optimal chemical composition, gives these materials a remarkable resistance to corrosion. In contrast to crystalline alloys, where the solubility of the elements is strictly limited, metal bottles allow an almost unlimited solubility of chemical components. This characteristic is the basis of atypical electronic behaviors at low temperatures, specific to these materials and difficult to reproduce in other systems.

The presence of metallic interatomic bonds in the structure of these alloys confers distinct properties compared to non-metallic glasses, including ductility and high breaking strength, without manifesting the brittle behavior characteristic of brittle materials. Due to these outstanding characteristics, massive amorphous alloys have found applicability in a wide spectrum of industrial and technological fields.



#### **Nanoporous structures**

Nanoporous structures are a distinct class of materials characterized by a three-dimensional network of pores that are generally less than 100 nm in size. These structures are distinguished by an extremely high specific surface area, a pronounced porosity and a controlled distribution of pore sizes, which gives them unique physicochemical properties. Nanoporous materials can be synthesized from a wide range of substances, including metals (e.g., porous gold and aluminum), silicates (such as mesoporous silica), polymers, and metal-organic hybrid materials

Nanoporous structures can be classified according to pore size into microporous (less than 2 nm), mesoporous (2–50 nm) and macroporous (>50 nm). Depending on the composition, they are divided into inorganic materials (such as silica and metals), organic (polymers) and hybrids. Synthesis methods may include wet chemical processes (sol-gel, self-assembly), electrochemical techniques (e.g., anodizing aluminum to obtain porous aluminum oxide), physical methods (electron beam deposition or ionization), and template-based replication techniques.

One of the most relevant examples for the manufacture of nanoporous structures is the controlled anodizing of aluminum, which makes it possible to obtain an orderly network of cylindrical, hexagonally arranged pores. This method is extremely versatile and allows fine control of parameters such as pore diameter, depth and spatial distribution.

Due to their high surface-to-volume ratio and high porosity, nanoporous materials have favorable characteristics for applications in areas such as controlled drug storage and delivery, molecular separations, chemical sensors, catalysis, tissue engineering and, last but not least, micro- and nanoelectromechanical devices (MEMS/NEMS).

For example, mesoporous silica is intensively studied for applications in personalized medicine, due to its ability to load and release drugs in a controlled manner. In the field of catalysis, nanoporous networks ensure efficient transport of reactants to active sites, contributing to improving the efficiency of chemical processes.

At the same time, porous anodized aluminum is widely used as a template for the synthesis of nanostructures, due to its well-defined architecture. These structures can be chemically functionalized for applications in microfluidics or as substrates for cell growth, in the context of tissue engineering.

Despite significant progress, research in the field of nanoporous structures faces a number of challenges. These include the difficulty of obtaining perfectly ordered structures over large areas, limitations in terms of the scalability of manufacturing processes and the thermal or chemical stability of materials in certain environments of use.

An emerging direction is the integration of nanoporous materials with other nanomaterials (e.g. metallic nanoparticles or graphene) to create advanced functional systems capable of responding to external stimuli. There is also a growing interest in the development of environmentally friendly, low-impact synthesis methods in line with the principles of green chemistry.

In conclusion, nanoporous structures represent a promising platform for the development of innovative solutions in numerous technological and biomedical fields. The ability to control architecture at the nanoscale opens up significant opportunities in the design of materials with adaptive functionality and superior performance. [17], [18], [19]

## Nanoporous materials obtained by dealloying amorphous metal alloys

The dealation process is an electrochemical reaction in which the less noble chemical elements in an alloy are removed or dissolved by the use of an oxidizing acid solution. Through this dissolving process, a nanoporous material is obtained. This nanoporous structure consists largely of noble elements and has no mechanical strength. The delineation process refers to the selective removal of one or more less noble elements from an alloy by the corrosion mechanism. For this reason, the loosening process is considered to be a destructive method in the electrochemical field. To date, this process has been used to produce metal porous structures such as Au, Ag, Pt, Cu and other alloys and solid solutions and metal bottles [20], [21], [22], [23], [24], [25]. To ensure the formation of a continuous porous structure, the amount of the noble element(s) should be between 20–45 at% [26], [27]. Other important parameters that play a crucial role during the dealding process include the critical corrosion potential, the composition of the alloy, the pH and also the temperature of the electrolyte[28].

The main advantages of amorphous precursors compared to crystalline alloy systems include the fact that they possess homogeneous composition and monolithic phase [29], thousands of metal bottles have been produced, which provide multiple precursors of [9] And also, most amorphous alloys



contain more than three different metals in their composition, which allows the formation of multielement nanoporous alloys [30]. During the tillage process of amorphous alloys, there are no granulation and crystal structure boundaries that provide active centers for the tillage process. Therefore, a change in the loosening mechanism may occur that provides access to advanced morphologies and properties of the final materials.

Regarding the mechanism of formation of porous metals when using amorphous precursors, various details are presented in the literature, including the diffusion coefficients of the elements that form the so-called ligament structures[31], [32].

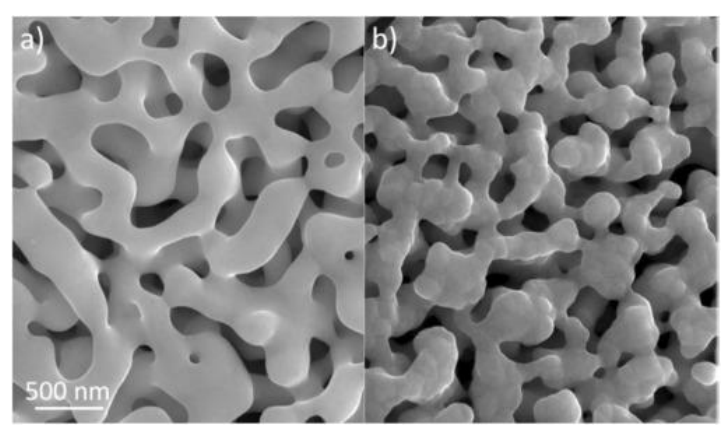


Figure 6 Close-up image of ligaments and pores obtained by unalloying a) the crystalline alloy Au31Cu41Zn12.8Mn15.2 and b) the amorphous alloy Au40Cu28Ag7Pd5Si20[33]

Although most studies show that due to the selective dissolution of amorphous alloys the resulting porous structure is nanocrystalline, there are also enough examples in the literature that reveal the preservation of the amorphous structure after the dealloying process of the obtained metallic glass [34], [35].

#### Hybrid additive manufacturing

Initially, Rajurkar et al. (1999) defined "hybrid machining" as a combination of two or more material removal processes [36]. However, this definition has been criticized for being too vaque, as many conventional manufacturing methods inherently involve multiple processes. To refine this definition, Kozak and Rajurkar (2000) pointed out that hybrid machining processes should exhibit performance characteristics that are significantly different from those of individual processes when performed separately[37]. Aspinwall et al. (2001) further clarified the concept, stating that hybrid machining involves the independent application of several processes on a single machine, while simultaneous application should be called "assisted" [38]. This distinction was important in delineating what constitutes hybrid production. In parallel with these developments in machining, the metal forming community has begun to use the term "hybrid" to describe processes that combine different forming techniques, such as extrusion and electromagnetic forming [39]. This indicates that the concept of hybridization was gaining ground in various production disciplines. In the early 2010s, the understanding of hybrid manufacturing expanded to include processes beyond machining. Nau et al. (2011) proposed that hybrid production should encompass the simultaneous use of different forms of energy in the same processing area [40]. This led to a definition proposed by the International Academy of Production Engineering (CIRP), which described hybrid manufacturing as involving the simultaneous and controlled interaction of process mechanisms and/or energy sources that significantly affect process performance. Zhu et al. contributed to the discourse by providing two definitions of hybrid manufacturing: a limited definition that focuses on competing processes in the same processing area, and a broad definition that encompasses the combination of manufacturing processes established in a new configuration [41]. The limited definition emphasizes the synergistic effect of combining in-situ processes, while the broad definition highlights the benefits of innovative combined approaches over conventional methods. Lauwers et al. (2014) revised these definitions and classified hybrid production into two main groups [42]. The first group (labeled "I") aligns with the limited definition, containing processes that combine energy sources/instruments for a synergistic effect. This group is divided into assisted trials (I.A) and



mixed trials (I.B). The second group (labeled "II") corresponds to the broad definition, in which processes act separately but are combined to increase efficiency and productivity. New hybrid manufacturing routes have emerged that combine additive manufacturing with conventional manufacturing. This requires a change in Lauwers et al.'s original classification to include new subgroups (II.A and II.B). Subgroup II.A refers to the controlled application of processes to mainly processed raw materials, while II.B, referred to as hybrid additive manufacturing (HAM), involves the application of processes to additively deposited materials. The overall vision of this new classification aims to improve the applicability of additive manufacturing by overcoming its limitations, such as low productivity and surface quality issues, while adding flexibility to traditional manufacturing processes. The evolution of the definition of hybrid manufacturing reflects a growing understanding of the complexities and synergies involved in combining different manufacturing processes. The discourse shifted from a narrow focus on machining to a broader perspective encompassing various manufacturing techniques, paving the way for innovative approaches that leverage the strengths of both additive and traditional methods [43].

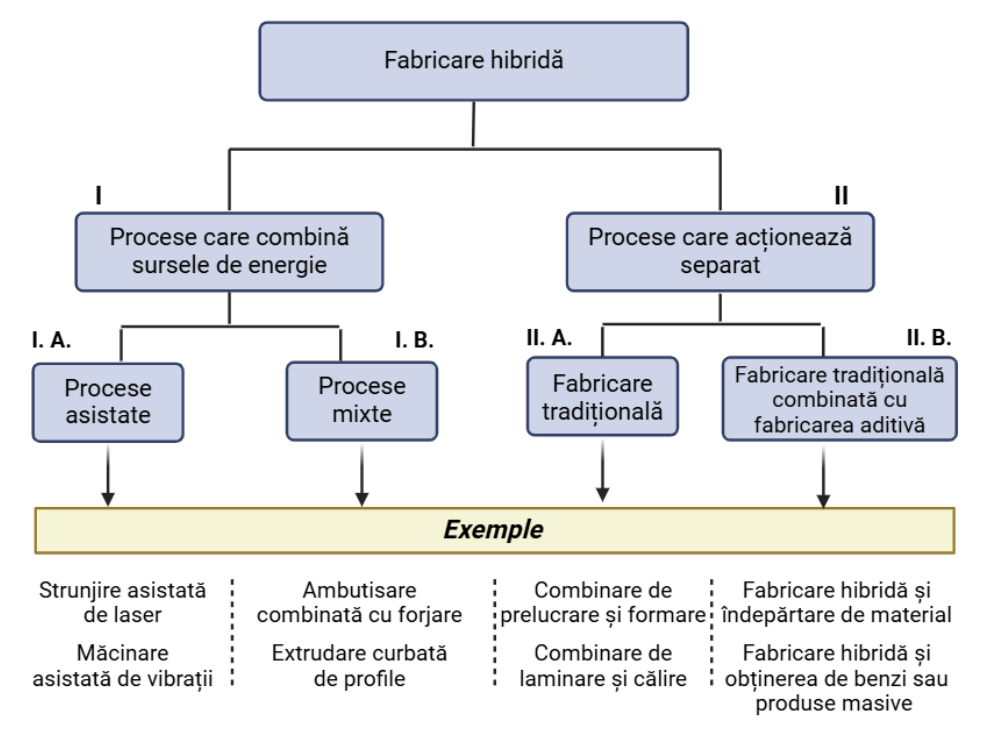


Figure 7 Classification of metal additive manufacturing (MAM) processes with widespread application in

Construction of three-dimensional metal parts

Hybrid metal additive manufacturing combines conventional manufacturing methods with additive manufacturing techniques to improve the production of complex metal components. Through this combination, the aim is to overcome individual limitations and obtain intrinsic advantages [44], [45].

Additive manufacturing, commonly known as 3D printing, builds objects layer by layer directly from a CAD model. These techniques allow for the creation of complex geometries and reduce material waste compared to conventional manufacturing methods. However, challenges such as surface roughness, residual stresses, and limited mechanical properties can arise in metal parts achieved by these methods.

To overcome these challenges, hybrid production systems have been developed. These systems integrate additive manufacturing processes with conventional techniques such as turning, milling or even forging. The hybrid approach allows in-situ machining during the additive process, resulting in improved surface quality, dimensional accuracy, and mechanical performance [46], [47].

The evolution of hybrid metal additive manufacturing has been driven by advances in both hardware and software. Innovations in laser and electron beam technologies, as well as the development



of multi-axis CNC machines, have expanded the capabilities of hybrid systems. In addition, software improvements in computer-aided design (CAD) and computer-aided manufacturing (CAM) have facilitated the seamless integration of additive and conventional techniques.

The applications in which hybrid metal additive manufacturing is used cover various industries, such as aerospace, automotive, medical, and tooling. In the aerospace industry, for example, hybrid manufacturing is used to produce lightweight, high-strength components with complex geometries that are difficult to achieve by conventional methods alone. In the medical field, it allows the manufacture of customized implants with precise surface finishes, improving biocompatibility and patient outcomes [45], [48], [49].

Despite its advantages, hybrid metal AM faces challenges that require further research and development. These include optimizing process parameters to ensure consistent quality, developing new materials compatible with hybrid systems, and reducing production costs to increase competitiveness with traditional manufacturing methods.

Hybrid metal additive manufacturing represents a significant advancement in the production of complex metal parts, combining the strengths of additive and traditional manufacturing techniques. Research and technological developments continue to expand its capabilities and applications, positioning it as a transformative approach in modern manufacturing.

## **Chapter 3 Purpose, Objectives, Experimental Program**

The purpose of this thesis is to develop the applications of families of amorphous non-ferrous metal alloys to the realization of components for electronic equipment, sensors, parts subjected to complex stresses using hybrid additive manufacturing methods.

In order to achieve the goal, the main objectives pursued are:

- development of amorphous metal alloys based on Cu-Ni-Sn-P with improved properties by additional alloy with Ga in the form of strips, rods and discs;
- obtaining nanoporous structures in the form of fruits, short bands from Cu-Ni-Sn-P-Ga by the process of hilling and obtaining powders by grinding;
- making polymer matrix composites reinforced with Cu-Ni-Sn-P-Ga particles or strips;
- characterization of them in terms of morphological, physical, mechanical, chemical properties;
- the development of new applications of these materials using various ways of realization that belong to the concept of hybrid additive manufacturing in areas where their properties contribute to the relevant improvement of product characteristics.

The experimental program will thus focus on research aimed at obtaining Cu-Sn-Ni-P amorphous alloys in different forms or integrated into other compositions, characterizing them from a structural, physical, mechanical, chemical point of view, as well as their use in the production of components, subject to complex stresses, produced by methods specific to hybrid additive manufacturing.



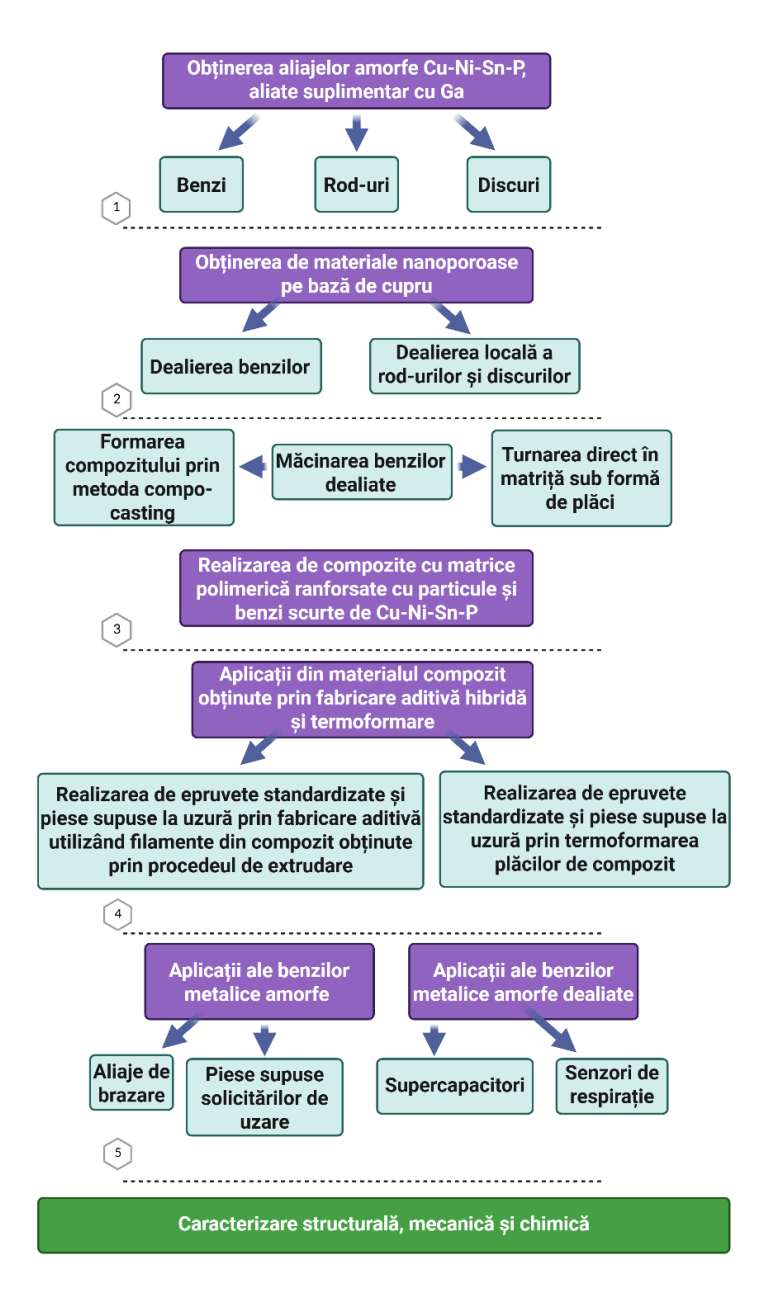


Figure 8 Experimental program



## Chapter 4 Equipment and methodology for experiments and testing

#### **Equipment for the experimental program**

The experiments carried out in order to achieve the assumed objectives required specific equipment and equipment, such as:

- Induction melting plant;
- Planetary Ball Mill (XQM);
- Mixing/homogenizing plant (Laboratory mixer, Rheomix R3000p/R3010p);
- Composite filament extruder (EvoFill device);
- Additive manufacturing equipment (Creality CR-10 Mini);
- Thermoforming equipment (Wickert WLP);
- Equipment for dealing.

## Equipment and apparatus for structural characterization and determination of mechanical and chemical properties

In order to characterize the structural and mechanical and chemical properties, the following were used:

- Difractometru de raze X (xPert Powder3 Panalytical);
- Installation for simultaneous thermal analysis (STA 449 F1 Jupiter, Netzsch);
- Microscop electronic de scanare (SEM Quanta FEG 250 FEI);
- Dispersed energy (EDX Quanta FEG 250 FEI) spectroscopy;
- Microscop optic (Olympus BX51M);
- Microdurimetru Vickers (Volpert Micro-Vickers Hardness Tester);
- Nanoindentor (Anton Paar Step 500);
- Tensile testing equipment (Zwick Roell Z005 device);
- Equipment for compression testing (LBG TC100 device);
- Wear test equipment (Pin-on-disk tribometer TR-20 micro).

## **Chapter 5 Experiments and Results**

#### Choice of compositional field

It has been shown that crystalline alloys of the Cu-Ni-Sn family are recommended for mechanical strength, high wear resistance and corrosion, having multiple uses including in robotics, electronics industry, aerospace.

The obtaining of amorphous alloys of this family is conditioned, in addition to technological constraints, by a favorable chemical composition consisting of the introduction of metalloids, the most used being phosphorus.

They were obtained in this way even in our laboratory [50] Cu-Ni-Sn-P metal bottles with improved mechanical properties in the form of strips, wires and thin bars by casting in metal molds with high conductivity.

In order to widen the dimensional range of these alloys, additional alloy with Gallium was used. This is a metal used in obtaining amorphous structures due to its characteristic of increasing the capacity of amorphization.

Gallium has a very low melting point. Its addition to an alloy tends to reduce the overall melting temperature, which allows the alloy to cool rapidly without crystallization and also favors the formation of an amorphous structure during solidification.

Given the specific requirements for an amorphous alloy and the desire to achieve the lowest possible melting temperature as well as a narrow solidification range, the following chemical composition of the primary alloy was chosen: **Cu75Ni6Sn5P14-xGax**. 3 variants of alloys were prepared.



No	х	Alloy
1	0	Cu75Ni6Sn5P14
2	4	Cu75Ni6Sn5P10Ga4
3	6	Cu75Ni6Sn5P8Ga6

## Obtaining amorphous metal alloys

Elaboration in the form of strips, fruits, discs

Elaboration of the primary alloy

The first stage in the manufacturing process consists of obtaining the primary alloy (master alloy). It was carried out using the installation developed in its own laboratories.

The technological process comprises the following steps: cutting the primary alloy bars into segments up to 40 mm, placing them in the crucible and fixing it, heating the alloy by induction, adjusting the speed of the cooling roller, positioning the crucible on top of the roller, applying an inert gas overpressure to the melt and ejecting it through the nozzle hole on the surface of the cooling roller

After weighing, the raw materials were fed into an alumina crucible and subjected to a five-fold

melting and remelting process to ensure the best possible homogenization of the alloy.



Figure 9 Smelting of raw materials

The casting of the primary alloy was carried out in a metal mold, resulting in bars with a diameter of  $\phi 10$  mm.



Figure 10 Casting form of primary alloy and solidified primary alloy

Obtaining amorphous alloys in the form of strips



The "melt-spinning" method was applied, which consists of ultra-fast cooling of the melt on the surface of a rotating cylinder.

The tests were carried out on all three types of Cu-Ni-Sn-P-Ga alloys.

Based on previous experiments on the development of strips by ultra-fast melt cooling [51], [52], [53], the following parameters were determined as optimal:

- topituria temperature: 800 °C;
- cooling roller speed: 4200 rpm;
- overpressure applied to melt: 0.3 atm;
- $\rightarrow$  nozzle-cooling roller surface distance: h = 0.6 0.8 mm;
- Angle of inclination of the crucible to the vertical: 8°.

Continuous strips with geometric uniformity, with a thickness of 25  $\mu$ m and a width of 1.5 mm, were obtained. The macroscopic appearance of these bands is shown in Figure 5.4.



Figura 11 Imagine macroscopică benzi metalice

The production of Bulk Metallic Glasses (BMGs) in the form of rods (bars) and discs required the use of casting molds designed for this purpose, made of Cu-Cr alloys, and provided with an additional cooling system. The molds consist of two symmetrical halves that are held in place with the help of four screws.



Figure 12. Copper mold for obtaining massive amorphous alloys in the form of discs



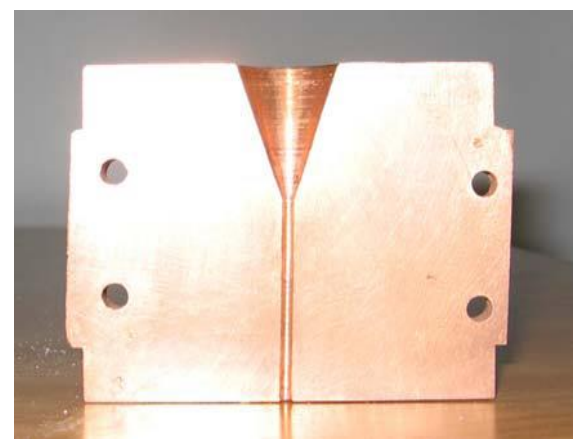


Figure 13. Copper mold for obtaining solid amorphous alloys in the form of fruits

Alloys with additional 4 % and 6 % Ga were tested.

For heating and melting the alloy, the same plant was used as in the case of strips. The molten alloys were ejected into a mold.

The result was to obtain fruits with diameters from 1 mm, 2 mm, respectively 3 mm and discourses with thicknesses of 1 mm and a diameter of 10 mm (fig. 5.7).



Figure 14. Macroscopic images of the metal fruits and the metal disc

The primary alloys developed have a crystal structure evidenced by X-ray diffraction. EDAX investigations certify the presence of the component chemical elements and the proposed concentrations.

For all 3 types of amorphous alloys developed in the form of strips, an amorphous structure was highlighted by X-ray diffraction analysis. In the case of obtaining massive amorphous alloys, X-ray diffraction analysis showed different structures. Thus, in the case of 1 and 2 mm nuts, and discs obtained from the Cu alloy $_{75\text{Ni}6\text{Sn}5\text{P1}0\text{Ga4}}$  An amorphous structure is certified. For 3 mm diameter bearings of the same alloy and 1 mm diameter bearings of Cu alloy $_{75\text{Ni}6\text{Sn}5\text{P8Ga6}}$ , the structure is partially amorphous, with spikes specific to crystalline compounds.

A further increase in the gallium proposition at the expense of phosphorus is not beneficial for obtaining massive amorphous alloys. It is concluded that the Cu alloy $_{75Ni6Sn5P10Ga4}$  The alloy supplemented with 4% gallium leads to increased amorphization capacity and will be used in experiments for application development. For the complete characterization of this alloy, the thermal stability and specific parameters were determined.

In order to determine the thermal stability and the specific parameters of the glass transition temperature  $T_g$ , and the crystallization temperature  $T_x$ , differential scanning calorimetry (DSC) was used. A Netzsch STA 441 Jupiter device was used. The glass transition temperature  $T_g$ , the crystallization temperature  $T_x$  and the melting temperature  $T_m$  were determined as the beginning temperatures of the peaks, during the heating of a sample weighing approximately 10 mg at a rate of 20 K · min-1 under a purified nitrogen flow rate at a flow rate of 40 ml · min-1.



#### **Obtaining nanoporous alloys**

As shown, to obtain nanoporous alloys, the most used process is selective dissolution following an electrochemical reaction also called dealing.

#### Dealloying of ribbons, rods and amorphous metal discs

The obtained  $Cu_{75}Ni_6Sn_5P_{10}Ga_4$  metal strips were subsequently subjected to a coating treatment in oxidizing acid solutions to selectively remove the nickel from the composition and obtain a nanoporous structure. For this step, three different acid solutions were used, namely sulfuric acid ( $H_{2SO4}$ ), hydrochloric acid (HCl) and hydrofluoric acid (HF). Different exposure conditions were also used, varying the exposure time, solution temperature and solution concentrations.

The delineation process carried out in H2SO4 solution at a concentration of 1M at 25 °C for 60 minutes leads to the best results. A large number of nanopores, evenly distributed on the surface of Cubased ribbons, were obtained compared to other treatment solutions.

In the case of untying the fruits and the metal disc, the samples of the composition  $Cu_{75}Ni_6Sn_5P_{10}Ga_4$  were subjected to a solution of  $H_2SO_4$  1M at a temperature of 55°C, for 336 hours (14 days). The samples analysed include three rods with diameters of 1 mm, 2 mm and 3 mm, as well as a metal disc with a diameter of 10 mm.

The SEM images shown in Figure 5.18 reveal a very porous structure, with pores varying at the nanoscale (about 100nm), evenly distributed in the structure of the amorphous metal strip.

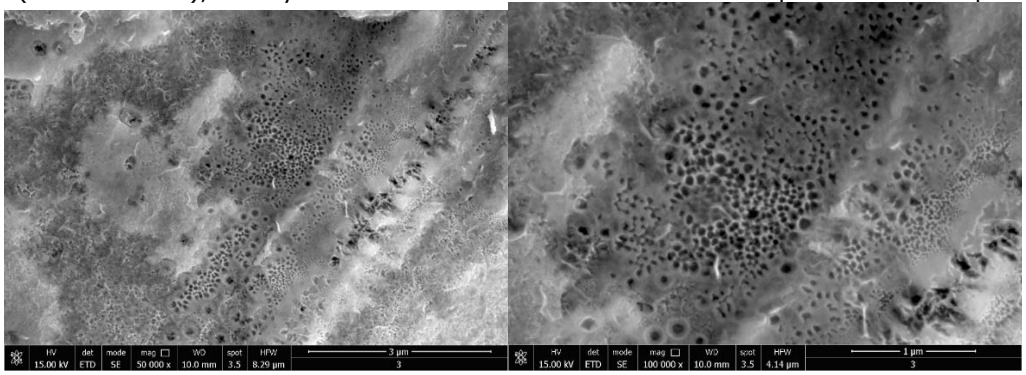


Figure 15. SEM images of the nanoporous structure obtained from dealloying

Microscopic analyses performed on the cross-sections of the fruits and discs show a porous area on the surface of samples with thicknesses between 165 and 237  $\mu m$ . The bluish tint of the reaction solution used in the delineation certifies the dissolution of the nickel-rich phases. In the case of 3 mm bars, the thickness of the affected layer is reduced due to the additional barrier to penetration of the acid solution by the increased volume of the material sample.

#### Structural Characterization of grinded ribbons

The powders obtained by grinding the  $Cu_{75}Ni_6Sn_5P_{10}Ga_4$  unalloyed bands were investigated using the scanning electron microscope.

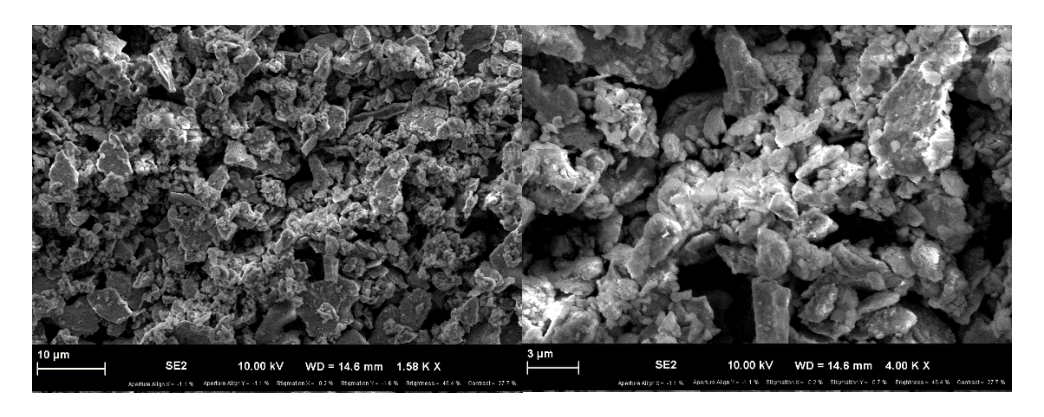




Figure 16. SEM images of the morphology of ground powders

From the SEM images shown in Figure 5.24, the morphology of the powders is characterized by an irregular shape, with particles having angular contours and rough surfaces. This morphology is typical for powders obtained by intense mechanical grinding, where fracturing processes dominate over plastic deformation processes. The particles do not exhibit spherical or ordered shapes, but rather fragmented aspects, which indicates a brittle breakage of the material during grinding.

#### **Composite Making by Compo-Casting Method**

In order to effectively fill the nanopores of a metal alloy de-alloyed with a polymer, it is essential to adapt the viscosity of the polymer so that it can fully penetrate the porous network of the reinforcer. The determination of the required viscosity can be done theoretically and/or experimentally, depending on the geometry and size of the pores.

The Washburn equation describes the dynamics of the advancement of a non-volatile liquid into a capillary tube (or into a moldable porous medium such as a network of cylindrical capillaries), under the action of surface tension forces and in the absence of external pressure.

$$L^2 = \frac{r \, \gamma \cos \theta}{2\eta} \cdot t$$

Where:

- L = the depth of penetration of the polymer into the pores;
- r = the radius of the pore;
- γ = surface tension of the molten polymer;
- $\theta$  = the contact angle between PLA and the metal alloy;
- η = viscosity of the molten polymer;
- t = penetration time

For the calculation of the process parameters, the pore size of approximately 99 nm measured on the obtained deallied amorphous bands was chosen. For the viscosity calculation we use the processing temperature for PLA at 200  $^{\circ}$ C.

The viscosity calculation using the Washburn equation will be like this:

$$\eta = \frac{r \gamma \cos \theta \cdot t}{2 L^2}$$

$$\eta = \frac{(49.5 \cdot 10^{-9}) \cdot (35 \cdot 10^{-3}) \cdot (0.87) \cdot 600}{2 \cdot (1 \cdot 10^{-6})^2}$$

$$\eta = \frac{(49.5)(35)(0.87)(600) \cdot 10^{-12}}{2 \cdot 10^{-12}}$$

$$\eta = \frac{905.347.5 \cdot 10^{-12}}{2 \cdot 10^{-12}}$$

$$\eta = 452.7 Pa \cdot s$$

The calculation shows that the viscosity required is about 450 steps for PLA to melt to 200  $^{\circ}$ C be able to penetrate 99 nm pores in a porous layer 1  $\mu$ m deep in 10 minutes. The actual viscosity of molten PLA is between 100 and 250 Pa·s, which means that PLA has a lower viscosity than the calculated threshold of 450 Pa·s. Thus, the polymer has the ideal viscosity to penetrate the 99 nm pores.



#### Obtaining filaments by extrusion of composite material

The composite material, represented by the polymeric matrix of PLA and reinforced with 10% powders and short strips of the alloy  $Cu_{75}Ni_6Sn_5P_{10}Ga_4$ , obtained by the composition-casting method was then shredded in order to be introduced into the extrusion equipment in order to obtain the filament necessary for additive manufacturing by the FDM method. Following the extrusion process, a filament with a slightly variable diameter of between 1.3-1.5 mm was obtained, which makes it suitable for further use in the additive manufacturing process by the FDM method.



Figure 17. Macroscopic image of the obtained filament

#### Manufacture of parts by additive manufacturing and thermoforming

For the 3D printing of the composite material, a layer height of 0.2 mm was chosen. The filling density was chosen at 75%, which resulted in a rectilinear filling model with a filling angle of 60°. Print speed has been set to 40 mm  $\cdot$  s<sup>-1</sup>. The nozzle temperature usedduring the printing process was 210 °C and the print bed temperature was set to 60 °C.



Figure 18. Macroscopic image of the distribution of particles and short bands in the 3D printed sample

Through the thermoforming process, specimens in the form of discs (fig. 5.36) were made of composite material made by the composite-casting method. The composite material, consisting of a matrix of polylactic acid (PLA) and copper-based amorphous metal powder, was placed in a preheated mold and subjected to heat treatment at a temperature of 170 °C. For a comparative study, a sample was also made only of polymeric material.





Figure 19. Thermoforming samples: left - composite material; right - PLA

To facilitate the complete formation of the parts in the mold and to ensure a uniform density, a pressure of about 10 MPa was applied. Following the application of the mentioned temperature and pressure, the pieces in the figure were obtained, with a circular geometry, having a diameter of 30 mm and a thickness of 5 mm.

#### Hardness testings

Alloys of the Cu-Ni-Sn-P-(Ga) family exhibit high strength properties in both crystalline and amorphous states. The hardness of these families of alloys is high, certifying that this family of alloys has some of the highest strength properties of non-ferrous alloys. At the same time, the amorphous state induces a slight increase in hardness.

#### **Nanoindentation**

In the experimental program, nanoindentation tests were carried out to have a more complete evaluation of the mechanical properties. The tests were performed using an NHT Antonn Parr nanoindenter and the Oliver & Pharr method was used to interpret the data.

## Amorphous Band Tests With 75Ni6Sn5P10Ga4

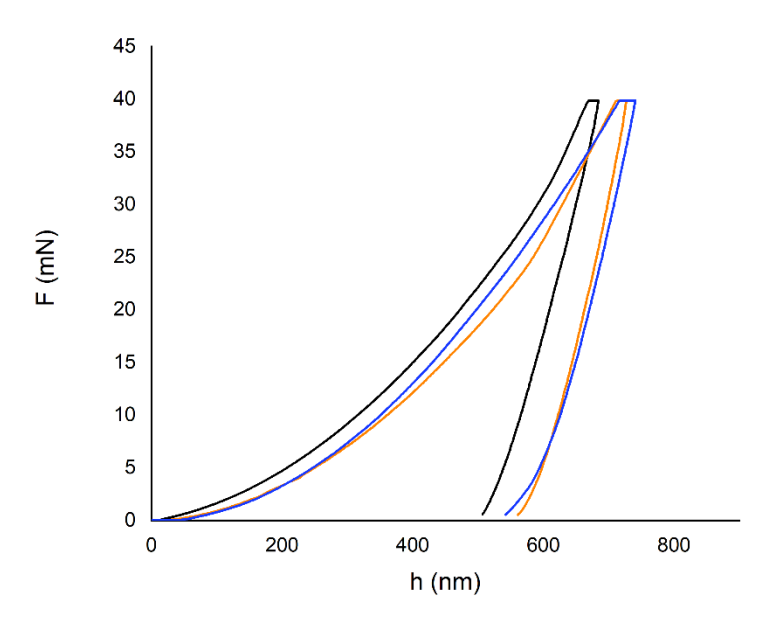


Figure 20. Charge-discharge curve on amorphous bands Cu75Ni6Sn5P10Ga4



## Tests on Amorphous Metal Strips Cu75Ni6Sn5P10Ga<sub>4</sub> Dealloyed

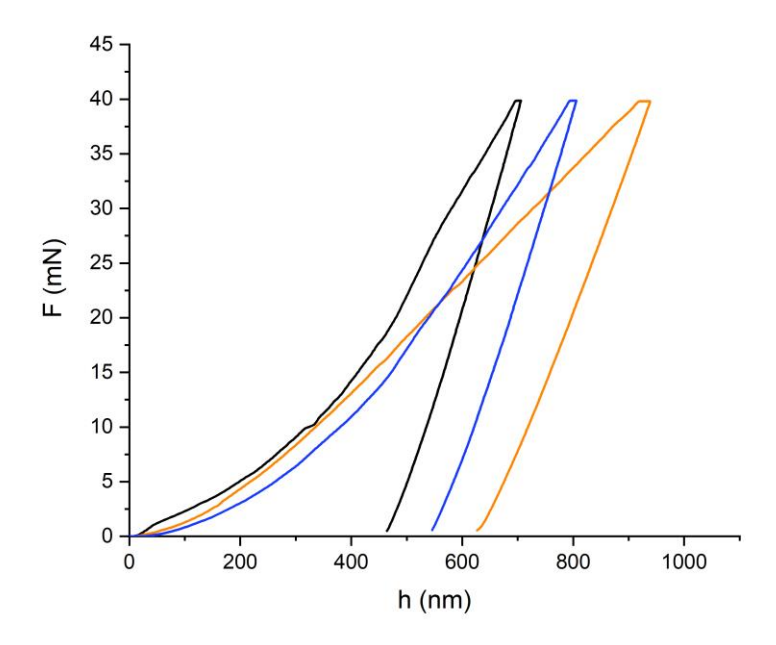


Figure 21. Loading-Unloading Curve Metal Strip Cu75Ni6Sn5P10Ga4 Unalloyed

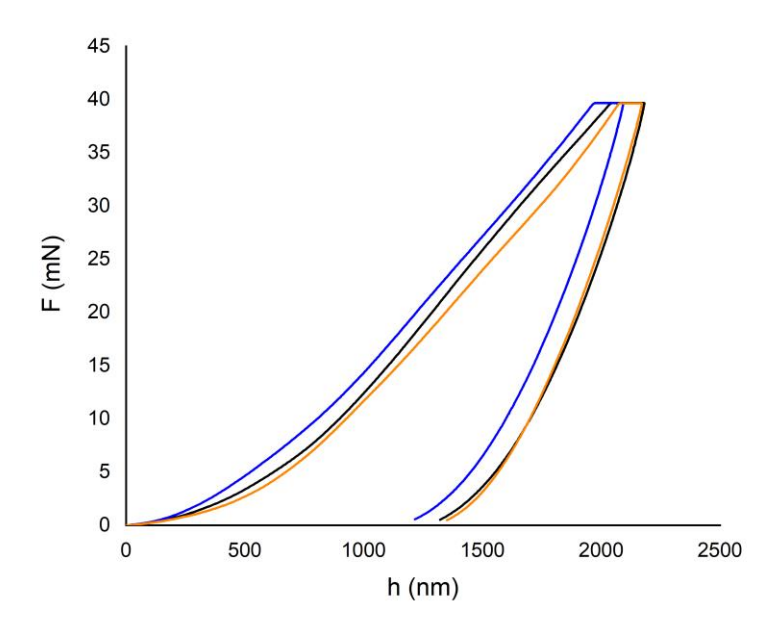


Figure 22. Loading-unloading curve 3D printed sample made of composite material



Nanoindentation tests on amorphous metal strips reveal values of indentation hardness of over 4000 MPa, and those of Vickers hardness around 500. Variations in hardness and mode of elasticity are attributed to inherent nanoscale heterogeneity in amorphous materials. In the case of dealloyed strips, a significant reduction in hardness and elasticity mode is observed, as a result of structural changes (partially crystallized) and high porosity, which may affect the use of nanoporous alloys in certain applications. The mechanical properties determined by nanoindentation in the case of the polymer matrix reveal the low hardness values and the modulus of elasticity, which is not usable for structural applications. In the case of reinforcement of the PLA polymer matrix with particles and short strips of the amorphous alloy, there is a spectacular improvement in hardness and modulus of elasticity and a complex behavior (combinations of elastic and plastic deformations during the test) of the composite under mechanical stress.

#### Tensile and compression test

Quasi-static mechanical tensile tests were performed to characterize the mechanical properties of the raw filaments. There are currently no specific standards available for filament testing. The filaments were tested under the elaborate conditions having a diameter of 1.3 mm. To obtain the reproducibility of the results, four samples of 70 mm in length were tested.

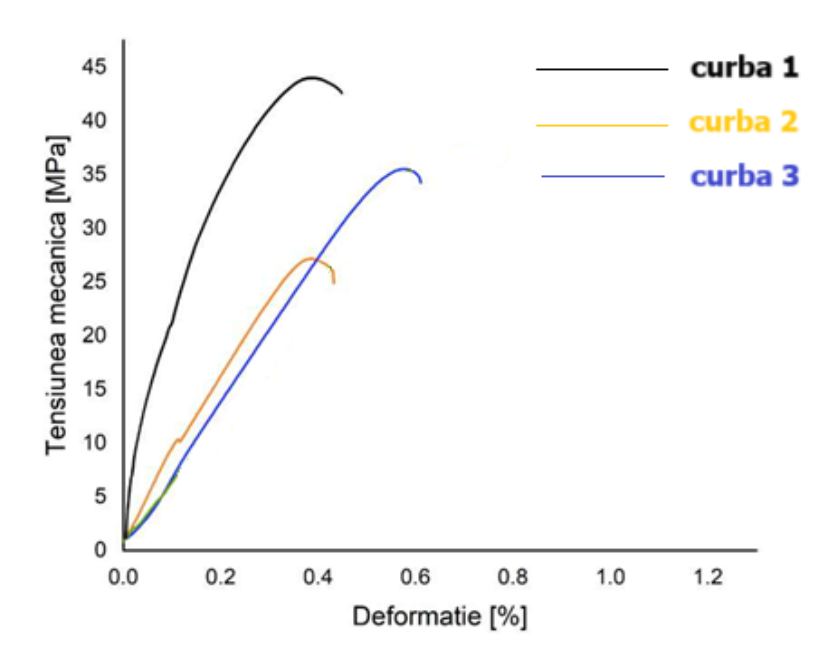


Figure 23. Stress-strain curve for composite filament

Curve 1 has a tensile strength of about 44 Mpa. The deformation at break is low, standing around 0.4%, which indicates a brittle and rigid behavior. The elastic region has a steep slope, suggesting a high modulus of elasticity and, implicitly, a higher rigidity than the other specimens. This behavior is characteristic of a rigid and brittle material, possibly a composite with a very low and well-dispersed metal powder content, where reinforcement contributes to rigidity without significantly compromising the initial mechanical characteristics of the polymer.

A notable decrease in tensile strength is also observed, in the case of curve 2, with a peak of around 27 Mpa. At the same time, the deformation at break is slightly higher, reaching about 0.45%. The rigidity of the material is noticeably lower. This profile may indicate a composite with a weak interface between the polymer and metal phases, where particles do not contribute effectively to charge transfer and, on the contrary, can act as crack initiators, reducing overall mechanical performance. Uneven dispersion or poor interface adhesion could explain these results.



Curve 3 stands out for an intermediate resistance, around 36 Mpa, but what differentiates it is the significantly higher deformation at break, of about 0.6%. Stiffness lies between the first two cases, suggesting a balance between flexibility and strength. This behavior can be associated with a composite formulation in which the metal powder is sufficiently well dispersed to contribute to energy absorption without drastically compromising the structural integrity of the material.

In order to evaluate the mechanical compressive behavior of the 3D printed composite, tests were carried out, both on the composite made of PLA reinforced with 10% powders and short strips of dealloy amorphous metal alloy, and on a sample of pure PLA, both being manufactured under the same conditions (density 70%, temperature 210°C).

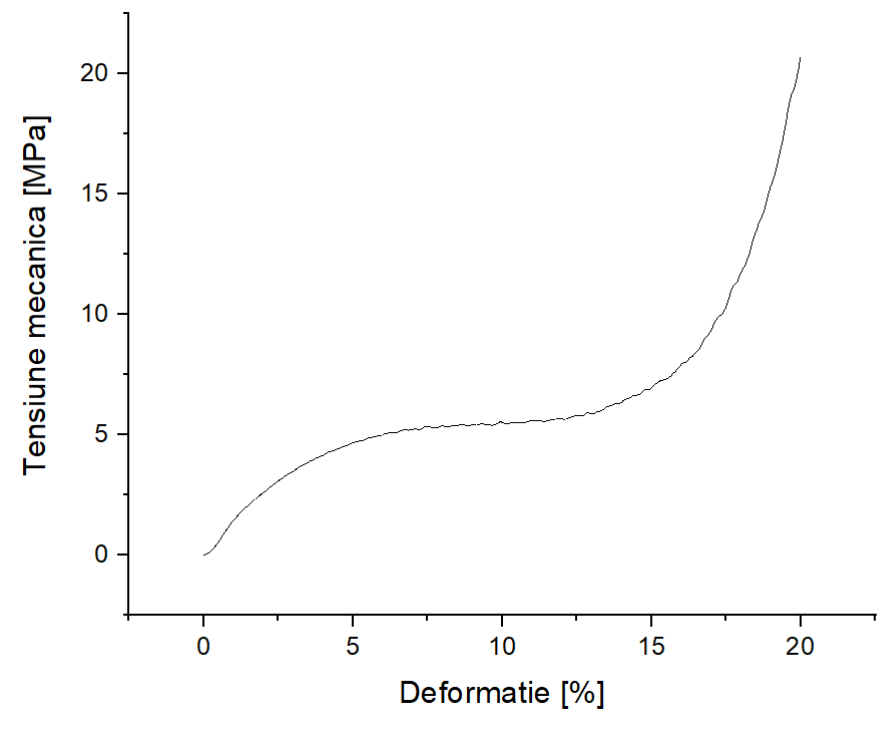


Figure 24. Stress-strain curve for 3D printed composite material

The compression curve of the composite made of PLA and 10% reinforcing (fig. 5.44) begins with a rapid increase in tension, which indicates an initial material-specific stiffness. In the first percentages of deformation, a concave area appears, typical of 3D printed materials by FDM, explained by the compaction of the internal voids resulting from the porous structure. As the deformation progresses, around 5-15% a plateau region appears, in which the tension remains almost constant. This behavior signals the controlled collapse of the walls of the internal cells and the absorption of energy through successive deformations of the microstructure.



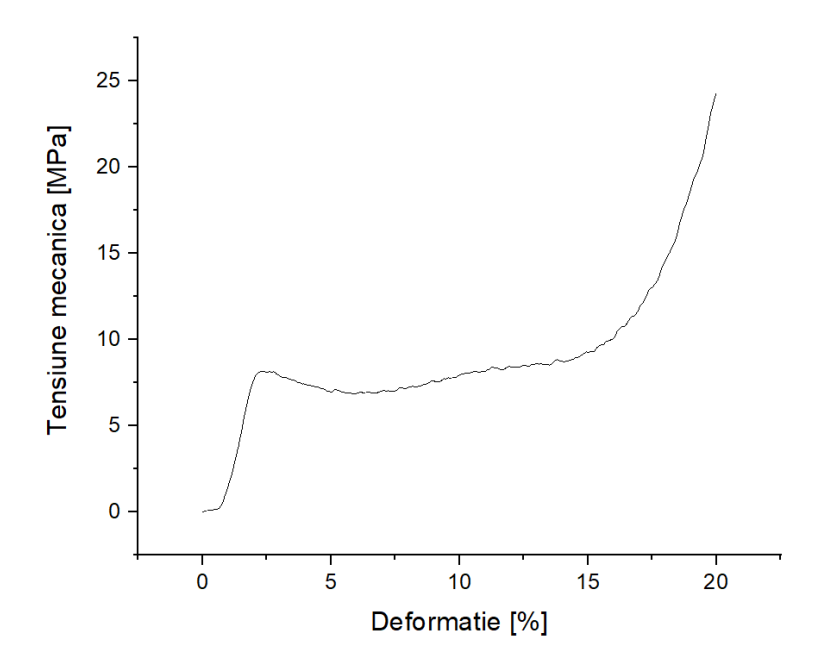


Figure 25. Stress-strain curve of PLA polymer material

The compression curve of the samples made of pure PLA (fig. 5.45) shows a behavior similar to that observed in the reinforced composite, but with some notable differences. Initially, the tension increases rapidly with the application of the load, reaching a peak of about 8.5 Mpa in the first 2% of strain. This increase is associated with the rigidity of the intact structure and the initial closure of microvoids. After this point, the curve enters a plateau region that extends to around 15% deformation. In this area, the voltage stabilizes at values of about 6.5–7 Mpa, indicating the progressive and controlled collapse of the porous internal structure.

#### **Corrosion test**

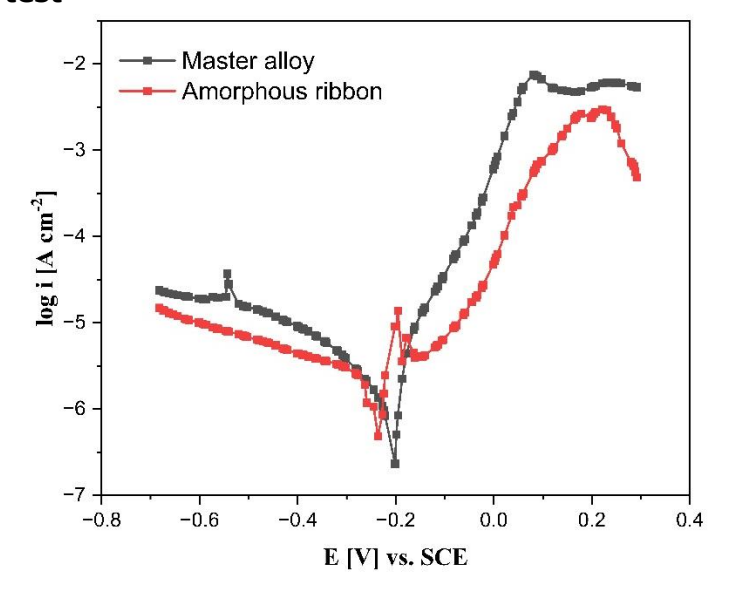


Figure 26. Electrochemical behavior analysis



The amorphous alloy strip Cu<sub>75</sub>Ni<sub>6</sub>Sn<sub>5</sub>P<sub>10</sub>Ga<sub>4</sub> exhibits significantly improved corrosion resistance compared to the master alloy according to electrochemical tests performed in 3.5% NaCl solution at room temperature. The bias curves highlight a lower corrosion current density and a more stable passive zone for the amorphous strip, indicating the formation of a thin and compact protective film. The amorphous, homogeneous structure without grain boundaries reduces the initiation and propagation of localized corrosion. Also, the alloying elements (Ni, Ga, P) help to improve passivation, making this alloy an attractive option for applications in aggressive salt environments.

## **Chapter 6 Applications**

#### **Applications of Amorphous Metal Ribbons**

Amorphous metal strips with the composition  $Cu_{75}Ni_{7}Sn_{5}P_{13}$  obtained in the form of continuous strips with a thickness of 25 µm, have proven to be highly effective brazing alloys for making high-quality capillary joints. The amorphous structure, devoid of crystalline grains and intermetallic phases, contributed essentially to the excellent behavior in the brazing process, regardless of the type of base material used (copper, stainless steel or combinations of these).

The behavior in the resistance brazing process highlighted the ability of the amorphous alloy to melt quickly, without significantly thermally affecting the base material. This behavior is visible in the case of copper platbands, where a continuous single-phase structure was obtained, without porosities or inclusions, at currents of 300-400 A and brazing times of 20-25 s. Also, the results obtained from the shear tests confirm the formation of mechanically robust joints, in which the breakage occurred in the copper, and not in the joint area.

#### Applications of Fully Dealloyed Metallic Ribbons as Breath Sensors

Respiration sensors are often used to detect specific gases in human or animal respiration (e.g. CO2, water vapor, volatile organic compounds - VOCs, or even ammonia in certain pathological conditions). Dealloyed amorphous alloys, having nanoporous structures with a large specific surface area, would be ideal for sensing due to the large number of active sites.

One of the promising applications of de-alloyed metal strips is their use in breathing sensors, demonstrated by testing them with a sensor based on gold interdigitated electrodes for respiration monitoring. Strips de-alloyed in  $H_{2SO4}$  solution were tested at different concentrations: 0.5M, 1M and 2M.

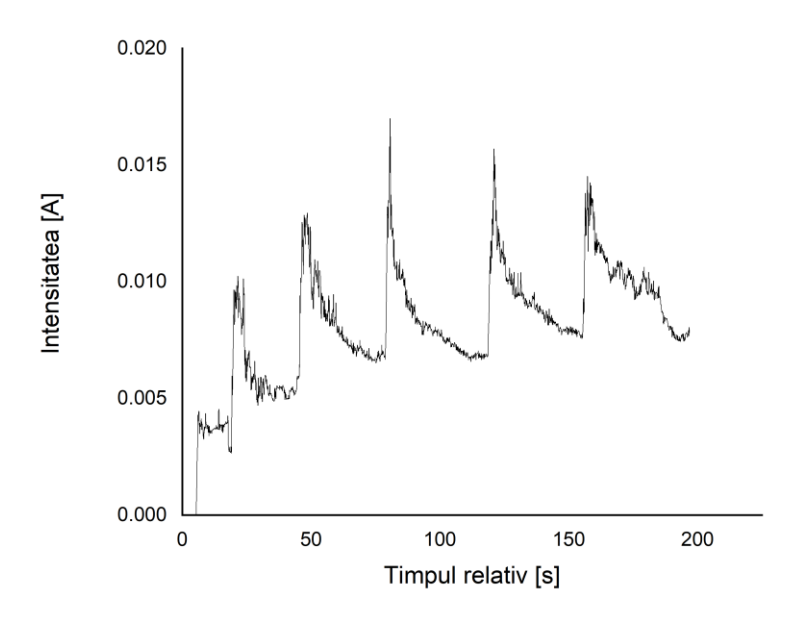


Figure 27. intensity-time variation for the amorphous metal bands of Cu<sub>75</sub>Ni<sub>6</sub>Sn<sub>5</sub>P<sub>10</sub>Ga<sub>4</sub> dealloyed in 1M H<sub>2SO4</sub>



In the case of the 1M H,  $_{2SO4}$  dealloyed band, the initial responses are very pronounced, some exceeding 0.018A, suggesting a particularly strong sensor response. However, a rapid and sharp decrease in the intensity of the peaks is observed, which indicates an accelerated desensitization. The base level is higher than in the other cases, but it has a decreasing trend during the measurement.

#### Applications of de-alloyed metal ribbons as supercapacitors

Amorphous alloys based on Cu-Ni-Sn-P-(Ga) are well known for their outstanding properties, which include good wetting of base materials, increased oxidation resistance, and dimensional stability during the heating process. These characteristics recommend them for industrial uses in brazing processes, especially for joining sensitive or porous metal materials, such as heat exchangers or catalytic converters. By their amorphous nature, these alloys allow the formation of uniform, thin bonding layers without the formation of unwanted intermetallic phases or brittle microstructures.

Interestingly, the chemical composition of Cu-Ni-Sn-P has recently demonstrated its versatility by extending its applicability to emerging areas such as electrochemical energy storage. The dealation process applied on the amorphous Cu-Ni-Sn-P-(Ga) bands led to the formation of high porosity structures (nanoporous copper – NPC) and to the development of an amorphous secondary phase based on tin pyrophosphate (Sn<sub>2</sub>P<sub>2</sub>O<sub>7</sub>), with pseudocapacitive properties. This hybrid architecture, made up of porous copper, copper oxide and Sn<sub>2</sub>P<sub>2</sub>O<sub>7</sub>, offers an advantageous combination of electrical conductivity, chemical stability and ion intercalation capacity, essential characteristics for materials active in supercapacitors.

#### Locally dealloyed rods and disc applications

Rods and discs made of Cu-Ni-Sn-P-(Ga) alloy, subjected to a local surface coating process, can be successfully used in advanced tribological applications, due to the microstructural and chemical changes that occur in the surface layer. Local loosening leads to the formation of a porous surface, with a rough topography and a varied chemical composition, capable of reducing friction and increasing wear resistance under conditions of intense mechanical stress.

This porous structure can act as a reservoir for solid or liquid lubricants, facilitating their uniform distribution during mechanical contact. Also, the elements present in the alloy, such as Sn and P, contribute to the formation of hard and wear-resistant phases, and Cu ensures good thermal conductivity, helping to efficiently dissipate the heat generated during friction. As a result, these materials can operate without external lubrication in demanding environments, such as those encountered in aerospace, automotive, or precision mechanical applications.

#### **Composite Applications**

The wear curves shown highlight a clear difference between the behavior of the plain PLA material and that of the powder-reinforced PLA composite and short strips of  $Cu_{75}Ni_6Sn_5P_{10}Ga_4$  amorphous metal alloy de-alloy. The black curve, related to simple PLA, indicates a marked wear over time, with a pronounced evolution in steps and oscillations, a sign that the material suffers rapid degradation and may be sensitive to load variations or unstable friction conditions. In contrast, the orange curve, associated with the reinforced material, shows a slower and smoother increase in wear, with reduced fluctuations, suggesting a more stable behavior in working mode. The difference in performance between the two materials confirms that the introduction of amorphous alloy particles and short fibers contributes significantly to improved durability and reduced wear, making the composite material a more suitable choice for demanding applications.



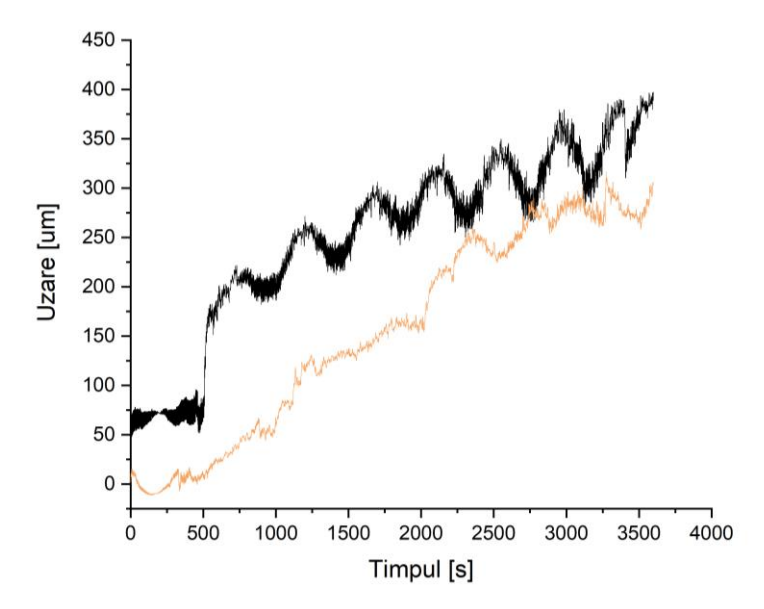


Figure 28. Wear curves for thermoformed samples: black - PLA; orange - composite material

#### **Chapter 7 Conclusions and own contributions**

The experimental research carried out for this purpose led to the following conclusions:

- 1. Master alloy primary alloys of the  $Cu_{75Ni6Sn5P14-xGax}$  family were developed by casting in the form of bars with a diameter of 10 mm, with x=0,2,4 both on the induction melting plant and on the electric arc vacuum remelting plant. The primary alloys have a crystalline structure evidenced by X-ray diffraction. EDAX investigations certify the presence of the component chemical elements and the proposed concentrations.
- 2. Non-ferrous amorphous alloys of the  $Cu_{75Ni6Sn5P14-xGax\ family\ were\ obtained}$ , with improved characteristics as a result of the alloy with Ga, in the form of strips, rods and discs, obtained by melt-spinning technique, respectively mold casting. By adding an additional 4% Ga, the amorphization capacity has been increased, making it possible to produce fruits with diameters up to 2 mm and discs with a thickness of 1 mm.

For all 3 types of amorphous alloys developed in the form of strips, an amorphous structure was highlighted by X-ray diffraction analysis. In the case of obtaining massive amorphous alloys, X-ray diffraction analysis showed different structures.

- 3. Nanoprobe materials were created by a process of dealing the amorphous metal strips  $Cu_{75}Ni_6Sn_5P_{10}Ga_4$  in oxidizing acid solutions for selective nickel removal. Similarly, fruits and discs of the same alloy were also subjected to the same process at a higher temperature and longer durations. EDX analyses supplemented with SEM analyses confirm the removal of Ni from the composition and the achievement of a porous structure with pore diameters close to 100 nm. The investigations also showed that the dealled bands exhibit a lower amount of amorphous phase and a higher degree of crystallinity.
- 4. Local nanoporous structures were obtained on massive amorphous alloys Microscopic analyses performed on the cross-sections of the fruits and discs show a porous area on the surface of the samples with thicknesses between 165 and 237  $\mu m$
- 5. Composites with polymer matrix and amophic particles and short strips have been made from the amorphous alloy  $Cu_{75Ni65n5P10Ga4}$ . The use of the compocasting method ensures a uniform distribution of the reinforcement in the matrix.
- 6. Following the extrusion process, a filament with a slightly variable diameter of  $1.3\,-\,1.5\,$  mm was obtained, which makes it suitable for further use in the additive manufacturing process by the FDM method.



7. Composite products have been made by <u>additive manufacturing</u> by the filament deposition method (FDM), using the filament obtained by the extrusion process. Through <u>the thermoforming process</u>, specimens were made in the form of composite discs made by the composite-casting method.

8. The mechanical tests carried out revealed:

Through the hardness test, it was highlighted that the amorphous state induces a slight increase in resistance properties.

Nanoindentation tests on amorphous metal strips reveal values of indentation hardness of over 4000 MPa, and those of Vickers hardness around 500. Variations in hardness and mode of elasticity are attributed to inherent nanoscale heterogeneity in amorphous materials. In the case of dealloyed strips, a significant reduction in hardness and elasticity mode is observed, as a result of structural changes (partially crystallized) and high porosity, which may affect the use of nanoporous alloys in certain applications. The mechanical properties determined by nanoindentation in the case of the polymer matrix reveal the low hardness values and the modulus of elasticity, which is not usable for structural applications. In the case of reinforcement of the PLA polymer matrix with particles and short strips of the amorphous alloy, there is a spectacular improvement in hardness and modulus of elasticity and a complex behavior (combinations of elastic and plastic deformations during the test) of the composite under mechanical stress.

The tensile tests performed on the composite material denote the specificity of the stress behavior of this material and the complexity of the interaction between the powder and the PLA matrix. The mechanical behavior differs depending on the concentration and distribution of the reinforcing material. At slightly lower concentrations, the composite has a high rigidity, and in the case of a very good dispersion of metal powders, it can lead to increased ductility and improved toughness.

Compression tests revealed the low strength of the composite compared to the polymer matrix due to its superior homogeneity.

- 9. Use of amorphous metal strips with the composition  $Cu_{75}Ni6Sn_5P_14$  obtained in the form of continuous strips with a thickness of 25 µm, as brazing alloys. The amorphous structure, devoid of crystalline grains and intermetallic phases, has made an essential contribution to the realization of high-quality capillary joints regardless of the type of base material used.
- 10. Realization of breathing sensors, based on de-allied metal bands demonstrated by testing them with a sensor based on gold interdigitated electrodes for respiration monitoring. The tilling process contributes significantly to increasing the sensitivity of the sensor, and the optimal concentration for maximum performance is  $1M\ H_2SO_4$ .
- 11. Use of amorphous Cu-Ni-Sn-P-(Ga) dealloyed bands as active materials for supercapacitors. The applied dealation process led to the formation of structures with high porosity and to the development of an amorphous secondary phase based on tin pyrophosphate  $(Sn_2P_2O_7)$ , with pseudocapacitive properties. This hybrid architecture, made up of porous copper, copper oxide and  $Sn_2P_2O_7$ , offers an advantageous combination of electrical conductivity, chemical stability and ion intercalation capacity, essential characteristics for materials active in supercapacitors.
- 12. Making the composite by incorporating amorphous alloy particles and short fibers contributes significantly to improved durability and reduced wear, making the composite material a more suitable choice for demanding applications. The wear curves highlight a clear difference between the behavior of the plain PLA material and that of the powder-reinforced PLA composite and short strips of Cu<sub>75</sub>Ni<sub>6</sub>Sn<sub>5</sub>P<sub>10</sub>Ga<sub>4</sub> amorphous metal alloy strips. The curve of the simple PLA indicates a marked wear over time, with a gradual evolution and pronounced oscillations, a sign that the material suffers rapid degradation and may be sensitive to load variations or unstable friction conditions. On the other hand, the curve associated with the composite material shows a slower and smoother increase in wear, with reduced fluctuations, which suggests a more stable behavior in working mode

Through the studies and researches carried out within this thesis, the following original contributions have been made:



- obtaining amorphous non-ferrous metal alloys based on Cu-Ni-Sn-P-Ga in the form of fruits, discs, strips, particles with improved characteristics as a result of alloy with Ga;
- carrying out detailed mechanical, chemical and structural investigations on the alloys and products obtained (XRD, DSC, SEM, micro-Vickers analyses, nanoindentation, corrosion tests and tensile and compression tests) that have certified properties that make them usable in different fields;
- the development of technological processes <u>specific to hybrid additive manufacturing</u> by including in the manufacturing cycle of the products obtained, the methods of compo-casting, extrusion, additive manufacturing, thermoforming;
- determination by calculation of the parameters of the manufacturing process of composites with polymer matrix and nanoporous reinforcer;
- realization of "breathing" sensors by unalloying elaborate amorphous alloys;
- manufacture of polymer matrix composites made of particle-reinforced PLA and short strips used in the manufacture of parts with mechanical strength and wear by processes specific to hybrid additive manufacturing.

As a result of the experiments carried out and the results obtained, new research directions in this field have emerged:

- 1. Development of new chemical compositions with high amorphization capacity in order to diversify the production of massive amorphous alloys (third generation of amorphous alloys).
- 2.Improving the characteristics of particle- and short-strip reinforced polymer composites to broaden the field of application by developing new manufacturing technologies and equipment.

#### Selective bibliography

- [1] F. C. Li *et al.*, "Amorphous–nanocrystalline alloys: fabrication, properties, and applications," *Mater. Today Adv.*, vol. 4, p. 100027, Dec. 2019, doi: 10.1016/j.mtadv.2019.100027.
- [2] H. Gleiter, "Nanocrystalline materials," *Prog. Mater. Sci.*, vol. 33, no. 4, pp. 223–315, Jan. 1989, doi: 10.1016/0079-6425(89)90001-7.
- [3] K. S. Kumar, H. Van Swygenhoven, and S. Suresh, "Mechanical behavior of nanocrystalline metals and alloys11The Golden Jubilee Issue—Selected topics in Materials Science and Engineering: Past, Present and Future, edited by S. Suresh," *Gold. Jubil. Issue Sel. Top. Mater. Sci. Eng. Past Present Future*, vol. 51, no. 19, pp. 5743–5774, Nov. 2003, doi: 10.1016/j.actamat.2003.08.032.
- [4] C. Suryanarayana and A. Inoue, "Metallic Glasses," 2012. doi: 10.1002/14356007.a16\_335.pub2.
- [5] M. L. Trudeau and J. Y. Ying, "Nanocrystalline materials in catalysis and electrocatalysis: Structure tailoring and surface reactivity," *Sel. Pap. TMS-AIME Symp. Struct. Prop. Nanophase Mater.*, vol. 7, no. 1, pp. 245–258, Jan. 1996, doi: 10.1016/0965-9773(95)00308-8.
- [6] A. M. Glezer and N. A. Shuryqina, Amorphous-nanocrystalline alloys. CRC Press, 2017.
- [7] J. Xiong, S.-Q. Shi, and T.-Y. Zhang, "Machine learning prediction of glass-forming ability in bulk metallic glasses," *Comput. Mater. Sci.*, vol. 192, p. 110362, May 2021, doi: 10.1016/j.commatsci.2021.110362.
- [8] D. Buzdugan, C. Codrean, M. Vodă, and V. A. Şerban, "Establishing the Glass Forming Ability of Ferromagnetic Bulk Amorphous Alloys Using a Mathematical Model Based on the Chemical Composition," *Solid State Phenom.*, vol. 188, pp. 11–14, 2012, doi: 10.4028/www.scientific.net/SSP.188.11.
- [9] W. H. Wang, C. Dong, and C. H. Shek, "Bulk metallic glasses," *Mater. Sci. Eng. R Rep.*, vol. 44, no. 2, pp. 45–89, Jun. 2004, doi: 10.1016/j.mser.2004.03.001.
- [10] M. L. F. Nascimento, L. A. Souza, E. B. Ferreira, and E. D. Zanotto, "Can glass stability parameters infer glass forming ability?," *J. Non-Cryst. Solids*, vol. 351, no. 40, pp. 3296–3308, Oct. 2005, doi: 10.1016/j.jnoncrysol.2005.08.013.



- [11] Y. Li, S. C. Ng, C. K. Ong, H. H. Hng, and T. T. Goh, "Glass forming ability of bulk glass forming alloys," Scr. Mater., vol. 36, no. 7, pp. 783–787, Apr. 1997, doi: 10.1016/S1359-6462(96)00448-4.
- [12] Z. P. Lu, H. Tan, S. C. Ng, and Y. Li, "The correlation between reduced glass transition temperature and glass forming ability of bulk metallic glasses," *Scr. Mater.*, vol. 42, no. 7, pp. 667–673, Mar. 2000, doi: 10.1016/S1359-6462(99)00417-0.
- [13] Z. P. Lu, Y. Li, and S. C. Ng, "Reduced glass transition temperature and glass forming ability of bulk glass forming alloys," *J. Non-Cryst. Solids*, vol. 270, no. 1, pp. 103–114, May 2000, doi: 10.1016/S0022-3093(00)00064-8.
- [14] C. Suryanarayana and A. Inoue, Bulk Metallic Glasses (2nd ed.). CRC Press, 2017.
- [15] A. A. Shirzadi, T. Kozieł, G. Cios, and P. Bała, "Development of Auto Ejection Melt Spinning (AEMS) and its application in fabrication of cobalt-based ribbons," *J. Mater. Process. Technol.*, vol. 264, pp. 377–381, Feb. 2019, doi: 10.1016/j.jmatprotec.2018.09.028.
- [16] W. Feng *et al.*, "Effect of Pouring Techniques and Funnel Structures on Crucible Metallurgy: Physical and Numerical Simulations," *Materials*, vol. 17, no. 19, 2024, doi: 10.3390/ma17194920.
- [17] M. H. Lee and D. J. Sordelet, "Nanoporous metallic glass with high surface area," Scr. Mater., vol. 55, no. 10, pp. 947–950, Nov. 2006, doi: 10.1016/j.scriptamat.2006.07.024.
- [18] "(PDF) ChemInform Abstract: Nanoporous Metals: Fabrication Strategies and Advanced Electrochemical Applications in Catalysis, Sensing and Energy Systems," *ResearchGate*, doi: 10.1039/c2cs35210a.
- [19] Q. Sang, S. Hao, J. Han, and Y. Ding, "Dealloyed nanoporous materials for electrochemical energy conversion and storage," *EnergyChem*, vol. 4, no. 1, p. 100069, Jan. 2022, doi: 10.1016/j.enchem.2022.100069.
- [20] D. V. Pugh, A. Dursun, and S. G. Corcoran, "Formation of nanoporous platinum by selective dissolution of Cu from Cu0.75Pt0.25," J. Mater. Res., vol. 18, no. 1, pp. 216–221, Jan. 2003, doi: 10.1557/JMR.2003.0030.
- [21] F. U. Renner, Y. Gründer, P. F. Lyman, and J. Zegenhagen, "In-situ X-ray diffraction study of the initial dealloying of Cu3Au(001) and Cu0.83Pd0.17(001)," Ninth Int. Conf. Surf. X-Ray Neutron Scatt., vol. 515, no. 14, pp. 5574–5580, May 2007, doi: 10.1016/j.tsf.2006.12.003.
- [22] J. R. Hayes, A. M. Hodge, J. Biener, A. V. Hamza, and K. Sieradzki, "Monolithic nanoporous copper by dealloying Mn–Cu," *J. Mater. Res.*, vol. 21, no. 10, pp. 2611–2616, Oct. 2006, doi: 10.1557/jmr.2006.0322.
- [23] C. Zhao, Z. Qi, X. Wang, and Z. Zhang, "Fabrication and characterization of monolithic nanoporous copper through chemical dealloying of Mg–Cu alloys," *Rolls. Sci.*, vol. 51, no. 9, pp. 2120–2125, Sep. 2009, doi: 10.1016/j.corsci.2009.05.043.
- [24] Z. Zhang, Y. Wang, Z. Qi, W. Zhang, J. Qin, and J. Frenzel, "Generalized Fabrication of Nanoporous Metals (Au, Pd, Pt, Ag, and Cu) through Chemical Dealloying," *J. Phys. Chem. C*, vol. 113, no. 29, pp. 12629–12636, Jul. 2009, doi: 10.1021/jp811445a.
- [25] Y.-W. Lin, C.-C. Tai, and I.-W. Sun, "Electrochemical Preparation of Porous Copper Surfaces in Zinc Chloride-1-ethyl-3-methyl Imidazolium Chloride Ionic Liquid," *J. Electrochem. Soc.*, vol. 154, no. 6, p. D316, Apr. 2007, doi: 10.1149/1.2724154.
- [26] Y. Ding and Z. Zhang, "Nanoporous Metals," in *Springer Handbook of Nanomaterials*, R. Vajtai, Ed., Berlin, Heidelberg: Springer Berlin Heidelberg, 2013, pp. 779–818. doi: 10.1007/978-3-642-20595-8\_21.
- [27] H.-J. Qiu, L. Peng, X. Li, H. T. Xu, and Y. Wang, "Using corrosion to fabricate various nanoporous metal structures," *Rolls. Sci.*, vol. 92, pp. 16–31, Mar. 2015, doi: 10.1016/j.corsci.2014.12.017.
- [28] K. Sieradzki, N. Dimitrov, D. Movrin, C. McCall, N. Vasiljevic, and J. Erlebacher, "The Dealloying Critical Potential," J. Electrochem. Soc., vol. 149, no. 8, p. B370, Jul. 2002, doi: 10.1149/1.1492288.
- [29] X. Luo, R. Li, L. Huang, and T. Zhang, "Nucleation and growth of nanoporous copper ligaments during electrochemical dealloying of Mg-based metallic glasses," *Rolls. Sci.*, vol. 67, pp. 100–108, Feb. 2013, doi: 10.1016/j.corsci.2012.10.010.
- [30] Z. Deng, C. Zhang, and L. Liu, "Chemically dealloyed MgCuGd metallic glass with enhanced catalytic activity in degradation of phenol," *Intermetallics*, vol. 52, pp. 9–14, Sep. 2014, doi: 10.1016/j.intermet.2014.03.007.



- [31] R. Li, N. Wu, J. Liu, Y. Jin, X.-B. Chen, and T. Zhang, "Formation and evolution of nanoporous bimetallic Ag-Cu alloy by electrochemically dealloying Mg-(Ag-Cu)-Y metallic glass," *Rolls. Sci.*, vol. 119, pp. 23–32, May 2017, doi: 10.1016/j.corsci.2017.02.017.
- [32] P. Rizzi, F. Scaglione, and L. Battezzati, "Nanoporous gold by dealloying of an amorphous precursor," *SI ISMANAM 2012*, vol. 586, pp. S117–S120, Feb. 2014, doi: 10.1016/j.jallcom.2012.11.029.
- [33] F. Scaglione, F. Celegato, P. Rizzi, and L. Battezzati, "A comparison of de-alloying crystalline and amorphous multicomponent Au alloys," *Intermetallics*, vol. 66, pp. 82–87, Nov. 2015, doi: 10.1016/i.intermet.2015.06.022.
- [34] R. Jiang et al., "Highly efficient amorphous np-PdFePC catalyst for hydrogen evolution reaction," Electrochimica Acta, vol. 328, p. 135082, Dec. 2019, doi: 10.1016/j.electacta.2019.135082.
- [35] S. Wang, C. Zhang, H. Li, and L. Liu, "Enhanced electro-catalytic performance of Pd-based amorphous nanoporous structure synthesized by dealloying Pd32Ni48P20 metallic glass," *Intermetallics*, vol. 87, pp. 6–12, Aug. 2017, doi: 10.1016/j.intermet.2017.04.002.
- [36] K. P. Rajurkar, D. Zhu, J. A. McGeough, J. Kozak, and A. De Silva, "New Developments in Electro-Chemical Machining," *CIRP Ann.*, vol. 48, no. 2, pp. 567–579, Jan. 1999, doi: 10.1016/S0007-8506(07)63235-1.
- [37] J. Kozak and K. P. Rajurkar, "Hybrid machining process evaluation and development," presented at the Proceedings of 2nd international conference on machining and measurements of sculptured surfaces, Keynote Paper, Krakow, 2000, pp. 501–536.
- [38] D. K. Aspinwall, R. C. Dewes, J. M. Burrows, M. A. Paul, and B. J. Davies, "Hybrid High Speed Machining (HSM): System Design and Experimental Results for Grinding/HSM and EDM/HSM," CIRP Ann., vol. 50, no. 1, pp. 145–148, Jan. 2001, doi: 10.1016/S0007-8506(07)62091-5.
- [39] A. Jäger, D. Risch, and A. E. Tekkaya, "Thermo-mechanical processing of aluminum profiles by integrated electromagnetic compression subsequent to hot extrusion," *Spec. Issue Impulse Form.*, vol. 211, no. 5, pp. 936–943, May 2011, doi: 10.1016/j.jmatprotec.2010.06.016.
- [40] B. Nau, A. Roderburg, and F. Klocke, "Ramp-up of hybrid manufacturing technologies," *Prod. Netw. Sustain.*, vol. 4, no. 3, pp. 313–316, Jan. 2011, doi: 10.1016/j.cirpj.2011.04.003.
- [41] Z. Zhu, V. G. Dhokia, A. Nassehi, and S. T. Newman, "A review of hybrid manufacturing processes state of the art and future perspectives," *Int. J. Comput. Integr. Manuf.*, vol. 26, no. 7, pp. 596–615, Jul. 2013, doi: 10.1080/0951192X.2012.749530.
- [42] B. Lauwers, F. Klocke, A. Klink, A. E. Tekkaya, R. Neugebauer, and D. Mcintosh, "Hybrid processes in manufacturing," *CIRP Ann.*, vol. 63, no. 2, pp. 561–583, Jan. 2014, doi: 10.1016/j.cirp.2014.05.003.
- [43] J. P. M. Pragana, R. F. V. Sampaio, I. M. F. Bragança, C. M. A. Silva, and P. A. F. Martins, "Hybrid metal additive manufacturing: A state-of-the-art review," *Adv. Ind. Manuf. Eng.*, vol. 2, p. 100032, May 2021, doi: 10.1016/j.aime.2021.100032.
- [44] M. Askari *et al.*, "Additive manufacturing of metamaterials: A review," *Addit. Manuf.*, vol. 36, p. 101562, Dec. 2020, doi: 10.1016/j.addma.2020.101562.
- [45] B. Barroqueiro, A. Andrade-Campos, R. A. F. Valente, and V. Neto, "Metal Additive Manufacturing Cycle in Aerospace Industry: A Comprehensive Review," *J. Manuf. Mater. Process.*, vol. 3, no. 3, 2019, doi: 10.3390/jmmp3030052.
- [46] J. Blindheim, T. Welo, and M. Steinert, "Investigating the Mechanics of Hybrid Metal Extrusion and Bonding Additive Manufacturing by FEA," Metals, vol. 9, no. 8, 2019, doi: 10.3390/met9080811.
- [47] D. D. Gu, W. Meiners, K. Wissenbach, and R. Poprawe, "Laser additive manufacturing of metallic components: materials, processes and mechanisms," *Int. Mater. Rev.*, vol. 57, no. 3, pp. 133–164, May 2012, doi: 10.1179/1743280411Y.0000000014.
- [48] W. E. Frazier, "Metal Additive Manufacturing: A Review," *J. Mater. Eng. Perform.*, vol. 23, no. 6, pp. 1917–1928, Jun. 2014, doi: 10.1007/s11665-014-0958-z.
- [49] A. Cohen, R. Chen, U. Frodis, M. Wu, and C. Folk, "Microscale metal additive manufacturing of multi-component medical devices," *Rapid Prototype. J.*, vol. 16, no. 3, pp. 209–215, Jan. 2010, doi: 10.1108/13552541011034889.
- [50] C. Stoian, "DEVELOPMENT OF COPPER-BASED AMORPHOUS BRAZING ALLOYS USED FOR WITH-WITH/STAINLESS STEEL JOINTS," Politehnica Timisoara, 2014.
- [51] C. Codrean, "Research on the process of hard bonding with amorphous alloys of stainless and refractory steels," 2005.